



Ethanol sensing properties of $\text{Bi}_{3.15}\text{Nd}_{0.85}\text{Ti}_3\text{O}_{12}$ films at low operating temperatures

Hong JIANG¹, Yong ZHANG²

1. Hunan Provincial Education Examination Board, Changsha 410006, China;
2. School of Physics and Optoelectronics, Xiangtan University, Xiangtan 411105, China

Received 9 November 2015; accepted 27 August 2016

Abstract: $\text{Bi}_{3.15}\text{Nd}_{0.85}\text{Ti}_3\text{O}_{12}$ (BNdT) films were deposited on Pt/Ti/SiO₂/Si(100) substrates by a metal organic decomposition (MOD) method, and annealed by a rapid thermal annealing process in oxygen atmosphere and in air, respectively. The crystalline structures and morphologies of BNdT films were characterized by X-ray diffraction and field-emission scanning electron microscopy, and the gas sensing properties were measured by monitoring its resistance at different gas concentrations. The results indicate that the BNdT films annealed in air are of porous microstructure and rough surface, and the annealing atmosphere has great influence on gas sensing properties. At an operating temperature of 100 °C, the BNdT films annealed in air are of high response value to 1×10^{-6} gaseous ethanol, and the detecting limit is as low as 0.1×10^{-6} . The corresponding response and recovery time is about 10 and 6 s, respectively. The results can offer useful guidelines for fabricating high performance ethanol sensors.

Key words: BNdT film; ethanol sensing properties; metal organic decomposition; annealing atmosphere; low operating temperature

1 Introduction

In recent years, perovskite-structured compounds (general formula ABO_3) have been attracted much attention due to their unique catalytic action [1], piezoelectric properties [2,3], and special performance in gas sensors [4–6]. Perovskite ABO_3 oxides, an important material family for the electronic and information technology, are also promising candidates for gas sensors [7]. Compared with simple metallic oxides, perovskite oxides are more stable and reliable [8]. In addition, the perovskite structure has two different sized cations, which makes it amenable to a variety of dopant additions. This doping flexibility allows for control of the transport and catalytic properties to optimize sensor performance for particular applications [9]. The ABO_3 -type oxide materials of rare-earth elements are highly defective and have oxygen deficient structures, in which the valence state of metal ions may be controlled by temperature, oxygen partial pressure and dopants [3,10,11]. Their sensitive and selective characteristics can be controlled by selecting suitable A and B atoms or

chemical dopants to give $\text{A}_{1-x}\text{A}'_x\text{B}_{1-y}\text{B}'_y\text{O}_3$ materials [12–15]. Hence, the ABO_3 -type oxide materials with special structures and morphologies have received considerable attention due to their special performance in gas sensors [16,17]. As can be foreseen, integrative devices with various applications will be vital for the next generation of electrical devices with more powerful functions and much smaller size [17]. For instance, TiO_2 may be chosen for fabricating photoelectric-gas sensors with special performance [18–20].

Up till now, the gas sensing materials worked at low temperature are favourable for fabricating low power consumption sensors, and several approaches are often used to lower the operating temperature of the gas sensing materials. One example is to add noble metal catalyst to the surface of the sensing materials [21,22]. The other is to reduce the diameter of the sensing materials, making it close to or smaller than the space-charge length (L_d) [23–26]. Hence, the current research mainly focuses on the development of reduced-temperature operation of the gas sensors for their further industrial applications. $\text{Bi}_{3.15}\text{Nd}_{0.85}\text{Ti}_3\text{O}_{12}$ (BNdT) thin film, as a good ferroelectric and

Foundation item: Project (51402250) supported by the National Natural Science Foundation of China; Project (2015JJ4046) supported by the Hunan Provincial Natural Science Foundation of China; Project (14B168) supported by the Scientific Research Fund of Hunan Provincial Education Department, China

Corresponding author: Yong ZHANG; Tel/Fax: +86-731-58292197; E-mail: zhangyong@xtu.edu.cn
DOI: 10.1016/S1003-6326(16)64451-5

piezoelectric material, has been widely investigated for their large remnant polarization ($2P_r$) and low leakage current [27–29]. However, relatively few reports for the gas sensing properties of BNdT thin film are available in the literatures. In this work, the ethanol sensing properties of BNdT thin films synthesized by metal organic decomposition (MOD) are investigated by exposing them to gaseous ethanol at different temperatures and concentrations. It is worth mentioning that this research may offer useful guidelines for the further industrial applications in fabricating high performance and low power consumption gas sensors.

2 Experimental

The BNdT films were fabricated on Pt/Ti/SiO₂/Si (100) substrates by metal organic decomposition (MOD). During the spin-coating procedure, the precursor solution for coating was prepared by dissolving bismuth nitrate, neodymium nitrate and titanium butoxide in proportion in glacial acetic acid at room temperature, with appropriate amount of acetylacetone added to stabilize the solution. 10% excess amount of bismuth nitrate was added to compensate for possible bismuth loss during annealing. The final concentration of precursor solution was 0.1 mol/L in BNdT, and the mix solution was spin-coated on substrate at 4000 r/min for 40 s. After the spin-coating procedure, the films were dried at 180 °C for 3 min, and pre-fired at 400 °C for 3 min to remove residual organic compounds. To investigate the effect of annealing atmosphere, the coated BNdT films were annealed by a rapid thermal annealing process for 10 min in oxygen atmosphere (BNdT-1) and in air (BNdT-2) at temperature of 750 °C, respectively. The crystalline structures of BNdT films were characterized by using a D/max 2500VK/PC X-ray diffraction (XRD) with Cu K_α radiation ($\lambda=1.5405$ Å), and the morphologies of BNdT films were recorded by FEI Quanta FEG 450 field emission scanning electron microscopy (FE-SEM).

Ethanol sensing characteristics were performed on a CGS-1TP intelligent gas sensing analysis system (Beijing Elite Tech Co., Ltd., China), and the schematic diagram of measure setup is shown in Fig. 1. The analysis system offers an external temperature control (from room temperature to 500 °C). The BNdT films with Pt/Ti/SiO₂/Si (100) substrates were placed on the temperature control and pre-heated at different operating temperatures for about 30 min. Two probes were pressed on the surface of BNdT films with Pt/Ti/SiO₂/Si (100) substrates by controlling the position adjustment in the analysis system. When the electrical signal is stable, ethanol gas is injected into the test chamber (18 L in volume) by a DGD-III dynamic gas distribution system (Beijing Elite Tech Co., Ltd., China). After the resistance

reached a new constant value, the test chamber was opened to recover the BNdT films in air. The resistance and response were collected and analyzed by the system in real time.

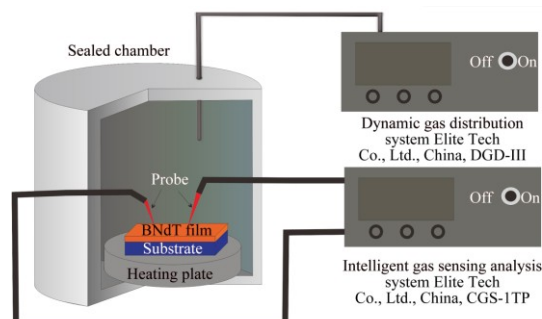


Fig. 1 Schematic diagram of measure setup

The response value (S) is designated as $S=R_a/R_g$, where R_a is the BNdT films resistance in air (base resistance) and R_g is its resistance in a mixture of ethanol gas and air. The time taken by the resistance to change from R_a to $R_a-90\%(R_a-R_g)$ is defined as response time when the ethanol gas is introduced to the BNdT films, and the time taken from R_g to $R_g+90\%(R_a-R_g)$ is defined as recovery time when the ambience is replaced by air.

3 Results and discussion

The XRD patterns of BNdT-1 and BNdT-2 are shown in Fig. 2. The peaks are indexed according to the standard diffraction pattern data of perovskite Bi₄Ti₃O₁₂ phase (JCPDS No. 73–2181). It is observed that all peaks of BNdT films coincided with those of Bi₄Ti₃O₁₂ films without any second phases. The BNdT-1 and BNdT-2 films consisting of a single phase of bismuth-layered perovskite are polycrystalline, without a preferred orientation, and both of them have good crystallinities. It is evident that the Nd³⁺ substitution does not affect the bismuth-layered structure of Bi₄Ti₃O₁₂ [30].

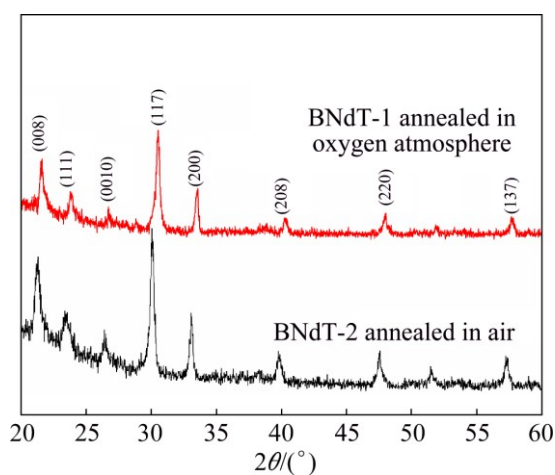


Fig. 2 XRD patterns of BNdT-1 and BNdT-2

The surface morphologies of BNdT films annealed in different atmospheres are shown in Fig. 3. Both BNdT-1 and BNdT-2 films are crack-free, uniform and adhere well on the substrates, and BNT-1 has a smooth and dense surface, as shown in Fig. 3(a). BNdT-2 (Fig. 3(b)), which exhibits a rough surface, is mostly composed of granular grains and the approximate diameter of grains is 100–300 nm. It is obvious that porous microstructure cannot be found in BNdT-1 but appears in BNdT-2, and the diameter of porous microstructure is about 50 nm. The appearance of porous microstructure and the rough surface are helpful for the increase of surface-to-volume ratio, which is beneficial to their sensing properties [31]. The oxygen concentration of annealing atmosphere is different between air and oxygen atmosphere. In the annealing process, Bi ions of the BNdT films are easy to volatile in a high temperature environment, thus the defects and oxygen vacancies are formed in the film [32]. When the BNdT films are annealed in oxygen atmosphere, the abundant oxygen in the environment can effectively restrain the formation of oxygen vacancies [33,34]. So, the different oxygen concentrations of annealing atmosphere lead to different morphologies between BNdT-1 and BNdT-2 films. The insets in Fig. 3 show

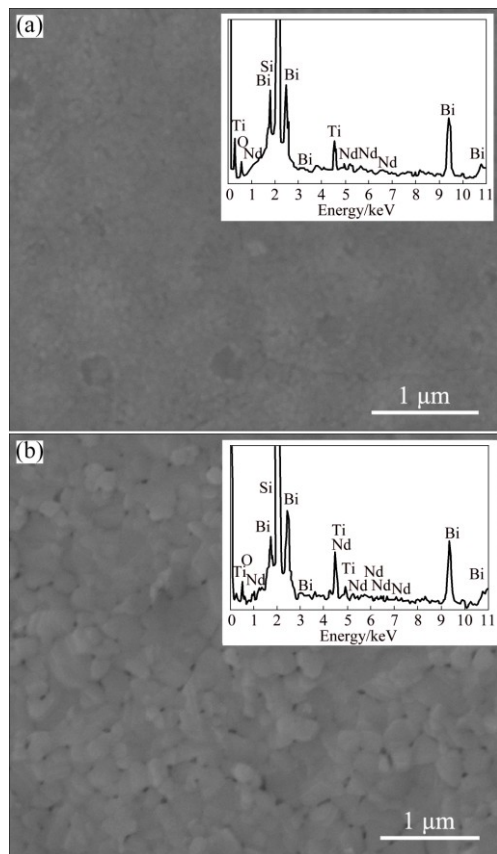


Fig. 3 FE-SEM images of BNdT-1 (a) and BNdT-2 (b) (The insets show the EDS patterns of BNdT films annealing in oxygen (a) and air (b) atmosphere)

the energy disperse spectroscopy (EDS) patterns. The Bi, Ti, Nd and O elements appear in the EDS pattern, which indicates that the as-prepared samples contain Bi, Ti, Nd and O elements. According to the above characterization results, the BNdT films with bismuth-layered perovskite structure are synthesized successfully.

To find out the optimization operating temperature for BNdT films, the responses of BNdT films to 1×10^{-6} ethanol can be calculated at eight different operating temperatures, and the curves of response vs temperature (T) are shown in Fig. 4. With increasing operating temperature, the response of BNdT films increases at $T \leq 100$ °C while decreases at $T > 100$ °C. The maximum response value of BNdT-2 is 6 at working temperature of 100 °C, which is larger than that of BNdT-1 ($S_g=5.5$) at the same temperature. The optimum working temperature of 100 °C for all BNdT films is applied in all investigations hereinafter.

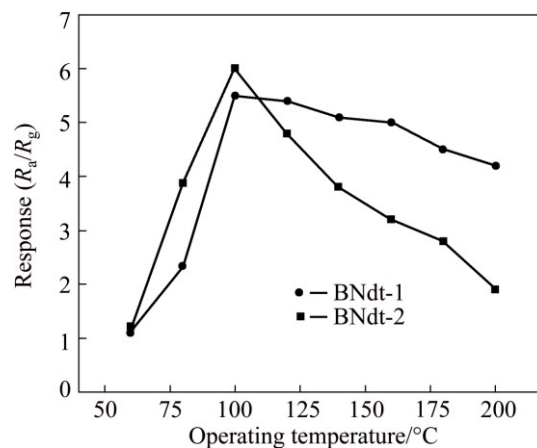


Fig. 4 Responses of BNdT-1 and BNdT-2 to 1×10^{-6} ethanol versus operating temperature

As a function of ethanol concentration, the responses of all BNdT films were measured at different ethanol concentrations of $(0.1-30) \times 10^{-6}$, and the correlation curves between the ethanol concentration and the response are shown in Fig. 5. It is obvious that the response increases gradually with the increasing ethanol concentration, and the response value of BNdT-2 is higher than that of BNdT-1 in the concentration range of $(0.1-30) \times 10^{-6}$. From Fig. 5, we can find that BNdT films are sensitive to gaseous ethanol at concentration down to 0.1×10^{-6} , and the responses of BNdT-2 are about 3, 6, 13, 16, 22, 29 and 35 for the ethanol gas at levels of 0.1×10^{-6} , 1×10^{-6} , 5×10^{-6} , 10×10^{-6} , 15×10^{-6} , 20×10^{-6} and 30×10^{-6} , respectively. Moreover, the insert in Fig. 5 shows the linear calibration curves in the ethanol concentration range of $(0.1-30) \times 10^{-6}$, which confirms that the concentration vs response curve of BNdT-2 is of the better linearity and higher slope comparing with it of BNdT-1. The good ethanol sensing properties of BNdT-2

are mainly due to the porous microstructure and the rough surface, which results in high surface-to-volume ratio of BNdT films. Thus, BNdT-2 is very promising for fabricating low power consumption gas sensors and for industrial applications. From the above discussion, the results show that BNdT-2 is of the higher response for ethanol gas than BNdT-1, so the response and recovery behaviors are studied for BNdT-2 in investigation hereinafter.

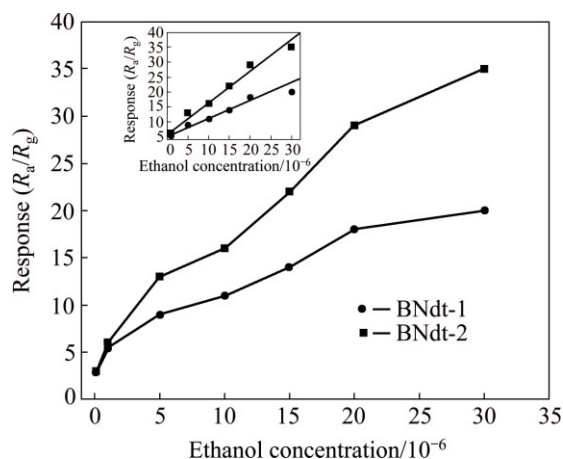


Fig. 5 Responses of BNdT-1 and BNdT-2 measured at various ethanol concentrations and 100 °C

Response and recovery behaviors are the important characteristics for evaluating the performance of the gas sensors, and transient response characteristics are measured by exposing BNdT-2 to the air and 1×10^{-6} gaseous ethanol as shown in Fig. 6. When BNdT-2 is exposed to 1×10^{-6} gaseous ethanol for 10 s, the transient response curve becomes stable while it takes 6 s for the transient response curve to return to the original value after the target vapour is replaced with air. The results suggest that BNdT-2 is of quick response and recovery behaviors for detecting gaseous ethanol, and the response and recovery time is 10 and 6 s, approximately.

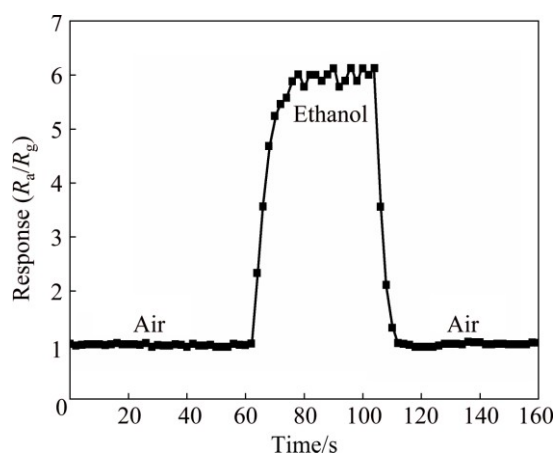


Fig. 6 Transient response characteristics of BNdT-2 to 1×10^{-6} ethanol at 100 °C

Generally, the metal oxide semiconductor (MOS) gas sensors work on the basis of the change of the electrical properties of the MOS, which results from the adsorption of the tested gas on the surface of the sensors. For the gas sensing materials, it is generally a surface controlled process that is responsible for the sensitivity [34]. The gas sensing mechanism for ethanol can be explained by the surface depletion [35,36] and the target gas chemisorption and desorption on the materials surface [37,38]. The schematic diagrams of gas sensing mechanism in air and ethanol gas are given in Fig. 7. The electrical conductance of the BNdT films is determined by the amount of electrons in its conduction band. The more the amount of electrons in the conduction band, the higher the conductivity of the BNdT films. When the BNdT films are exposed to air, oxygen molecules are adsorbed on the surface of BNdT films to form $O^{\delta-}$ (O^{2-} , O^- and O_2^-) oxygen negative ions species by capturing electrons from the conduction band (Figs. 7 (a) and (b)). The oxygen species adsorbed on the surface of BNdT films form a rather thick depletion region [24]. If the ethanol vapor does not adsorb at all or only physically adsorb on the surface of the BNdT films, there are no electrons exchanged between the BNdT films and the ethanol vapor molecules. Hence, the conductivity of the BNdT films remains the same level without the ethanol vapor. When the BNdT films are exposed to ethanol vapor at an operating temperature of 100 °C, the ethanol molecular reacts with the surface $O^{\delta-}$ oxygen negative ions species and release electrons which will migrate to the conduction band of the BNdT films, resulting in the reduction of the amount of surface adsorbed oxygen species (Figs. 7 (c) and (d)). As a result, the depletion layer becomes thin and the electrical conductivity increases (i.e., the decrease in the resistance) [39,40].

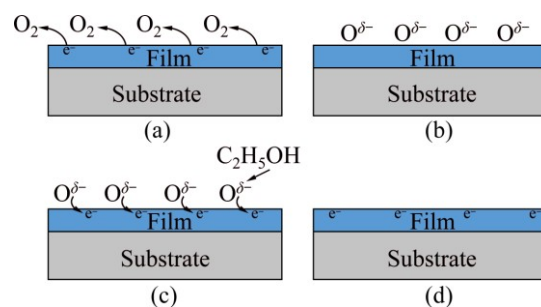


Fig. 7 Schematic diagrams of gas sensing mechanism: (a) Exposed to air; (b) $O^{\delta-}$ ions adsorbed; (c) Exposed to ethanol vapor; (d) Release electrons to BNdT films

Compared with BNdT-1, BNdT-2 owns improved and much better sensing performance. Two aspects can be referred to explain these sensing improvements. Firstly, the oxygen vacancy in the BNdT films acts as an electron donor, which provides electrons to conduction

band of BNdT films [41]. Many oxygen molecules can be adsorbed (or desorbed) in oxygen vacancy, and the increase of oxygen vacancy can improve the oxidation activity for reductive gas in low temperature [42,43]. When the BNdT films are annealed in oxygen atmosphere, the formation of oxygen vacancy is restrained, but the concentration of oxygen vacancy will increase while annealing in air because bismuth ion volatilizes from BNdT films during annealing [32]. Moreover, good crystallinity, which is obtained by the suitable preparation technology, can greatly change the gas sensing properties. Hence, the enhanced crystal structure of BNdT-2 with many oxygen vacancies can improve the ethanol sensing properties, such as low operating temperature and high response for ethanol detection [44,45]. Simultaneously, porous materials based on their structural characteristics (ordered pore distributions, high pore volumes and high surface areas) combined with the possibility to process them in various shapes (calibrated spherical powders, thin films, membranes, and monoliths) have attracted much research interest in sensor application developing its potential applications in recent decades. For semiconductor gas sensors, the porosity of sensing films is a vital parameter [46–48], and porous sensing films can facilitate gas diffusion deeply inside the films and reach high gas response [49,50]. The unique porous architecture can provide abundant active sites to the environment [51,52], and larger accessible surface together with convenient transport of gas can be benefited from the porous structure [53,54]. ZHANG et al [55] found that the destruction of the porous microstructure has negative effects on gas response due to the decrease of the porosity. Therefore, good sensing properties of BNdT-2 can be attributed to the good crystal structure of BNdT-2 with many oxygen vacancies and high porosity of the films, and these results also indicate the method for sensing improvement based on BNdT materials in the future.

4 Conclusions

1) The BNdT films are synthesized by MOD method, and annealed by a rapid thermal annealing process in oxygen atmosphere and in air, respectively. The crystalline structures, the morphologies and the component of elements of BNdT films are characterized by using XRD, FE-SEM, and EDS. The BNdT films annealed in air are of porous microstructure and rough surface. The appearance of porous microstructure and rough surface are helpful for the increase of surface-to-volume ratio, which is beneficial to their sensing properties.

2) BNdT-2 is of low operating temperature (100 °C),

and the detecting limit is as low as 0.1×10^{-6} . It is of high response ($S_g=6$) to 1×10^{-6} gaseous ethanol and the response and recovery time is 10 and 6 s, respectively. The results indicate that the BNdT annealed in air is of better gas sensing properties than that annealed in oxygen atmosphere. This work offers a promising material for fabricating low power consumption gas sensors.

References

- [1] LEVASSEUR B, KALIAGUINE S. Methanol oxidation on LaBO₃ (B=Co, Mn, Fe) perovskite-type catalysts prepared by reactive grinding [J]. *Applied Catalysis A: General*, 2008, 343: 29–38.
- [2] ZHOU Chang-rong, FETEIRA A, SHAN Xu, YANG Hua-bin, ZHOU Qin, CHENG Jun, LI Wei-zhou, WANG Hua. Remarkably high-temperature stable piezoelectric properties of Bi(Mg_{0.5}Ti_{0.5})O₃ modified BiFeO₃-BaTiO₃ ceramics [J]. *Applied Physics Letters*, 2012, 101: 032901.
- [3] HUANG Xiao-jun, YAN Xin, WU Hai-yan, FANG Ying, MIN Ya-hong, LI Wen-sheng, WANG Shuang-yin, WU Zhen-jun. Preparation of Zr-doped CaTiO₃ with enhanced charge separation efficiency and photocatalytic activity [J]. *Transactions of Nonferrous Metals Society of China*, 2016, 26: 464–471.
- [4] ZHANG Yong, ZHENG Xue-jun, ZHANG Tong, GONG Lun-jun, DAI Shun-hong, CHEN Yi-qiang. Humidity sensing properties of the sensor based on Bi_{0.5}K_{0.5}TiO₃ powder [J]. *Sensor and Actuators B: Chemical*, 2010, 147: 180–184.
- [5] ZHANG Yong, ZHENG Xue-jun, ZHANG Tong. Characterization and humidity sensing properties of Bi_{0.5}Na_{0.5}TiO₃-Bi_{0.5}K_{0.5}TiO₃ powder synthesized by metal-organic decomposition [J]. *Sensor and Actuators B: Chemical*, 2011, 156: 887–892.
- [6] YAO Peng-jun, WANG Jing, CHU Wen-ling, HAO Yu-wen. Preparation and characterization of La_{1-x}Sr_xFeO₃ materials and their formaldehyde gas-sensing properties [J]. *Journal of Materials Science*, 2013, 48: 441–450.
- [7] OBAYASHI H, SAKURAI Y, GEJO T. Perovskite-type oxides as ethanol sensors [J]. *Journal of Solid State Chemistry*, 1976, 17: 299–303.
- [8] YU Xue-lian, WANG Yu, HU Yong-ming, CAO Chuan-bao, CHAN H L W. Gas-sensing properties of perovskite BiFeO₃ nanoparticles [J]. *Journal of the American Ceramic Society*, 2009, 92: 3105–3107.
- [9] FERGUS J W. Perovskite oxides for semiconductor-based gas sensors [J]. *Sensor and Actuators B: Chemical*, 2007, 123: 1169–1179.
- [10] AKHTAR M J, AKHTAR Z N, DRAGUN J P, CATLOW C R A. Electrical conductivity and extended X-ray absorption fine structure studies of SrFe_{1-x}Nb_xO₃ and BaFe_{1-x}Nb_xO₃ systems [J]. *Solid State Ionics*, 1997, 104: 147–158.
- [11] YAN Xin, ZHAO Cui-lian, ZHOU Yi-long, WU Zhen-jun, YUAN Jian-min, LI Wen-sheng. Synthesis and characterization of ZnTiO₃ with high photocatalytic activity [J]. *Transactions of Nonferrous Metals Society of China*, 2015, 25: 2272–2278.
- [12] PHAWACHALOTORN C, SANGUANRUANG O, ISHIHARA T. Highly selective amperometric sensors for carbon monoxide detection in exhaust gas [J]. *Sensor and Actuators B: Chemical*, 2012, 161: 635–640.
- [13] GHASDI M, ALAMDARI H. Highly sensitive pure and Pd-doped LaFeO₃ nanocrystalline perovskite-based sensor prepared by high energy ball milling [J]. *Advanced Materials Research*, 2012, 409: 486–491.

- [14] MAQBOOL A, HUSSAIN A, RAHMAN J U, PARK J K, PARK T G, SONG J S, KIM M H. Ferroelectric and piezoelectric properties of SrZrO₃-modified Bi_{0.5}Nd_{0.5}TiO₃ lead-free ceramics [J]. Transactions of Nonferrous Metals Society of China, 2014, 24: s146–s151.
- [15] CHOE Y, SEO J, LEE K, LEE M, HWANG H. Cr-poisoning under open-circuit condition in LaNi_{0.6}Fe_{0.4}O_{3-δ}-based nano composite cathodes for solid oxide fuel cells prepared by infiltration process [J]. Transactions of Nonferrous Metals Society of China, 2016, 26: 1367–1372.
- [16] HU Y, TAN O K, PAN J S, HUANG H, CAO W. The effects of annealing temperature on the sensing properties of low temperature nano-sized SrTiO₃ oxygen gas sensor [J]. Sensor and Actuators B: Chemical, 2005, 108: 244–249.
- [17] ZHANG Yong, ZHENG Xue-jun, ZHANG Tong, SUN Jing, BIAN Yan, SONG Jie. Gas sensing properties of coral-like Bi_{0.5}K_{0.5}TiO₃ powders synthesized by metal-organic decomposition [J]. Measurement Science & Technology, 2011, 22(11): 115205.
- [18] LIU Hong-yan, GAO Lian. Synthesis and properties of CdSe-sensitized rutile TiO₂ nanocrystals as a visible light-responsive photocatalyst [J]. Journal of the American Ceramic Society, 2005, 88: 1020–1022.
- [19] PARK J Y, SONG S J, WACHSMAN E D. Highly sensitive/selective miniature potentiometric carbon monoxide gas sensors with titania-based sensing elements [J]. Journal of the American Ceramic Society, 2010, 93: 1062–1068.
- [20] CAO Guo-jian, CUI Bo, WANG Wen-qi, TANG Guang-ze, FENG Yi-cheng, WANG Li-ping. Fabrication and photodegradation properties of TiO₂ nanotubes on porous Ti by anodization [J]. Transactions of Nonferrous Metals Society of China, 2014, 24: 2581–2587.
- [21] WANG H T, KANG B S, REN F, TIEN L C, SADIK P W, NORTON D P, PEARTON S J, LIN J. Hydrogen-selective sensing at room temperature with ZnO nanorods [J]. Applied Physics Letters, 2005, 86(24): 243503.
- [22] TIEN L C, SADIK P W, NORTON D P, VOSS L F, PEARTON S J, WANG H T, KANG B S, REN F, JUN J, LIN J. Hydrogen sensing at room temperature with Pt-coated ZnO thin films and nanorods [J]. Applied Physics Letters, 2005, 87(22): 222106.
- [23] KIM Y S, HA S C, KIM K, YANG H, CHOI S Y, KIM Y T, PARK J T, LEE C H, CHOI J, PAEK J, LEE K. Room-temperature semiconductor gas sensor based on nonstoichiometric tungsten oxide nanorod film [J]. Applied Physics Letters, 2005, 86(21): 213105.
- [24] HUANG Hui, TAN O K, LEE Y C, TRAN T D, TSE M S, YAO X. Semiconductor gas sensor based on tin oxide nanorods prepared by plasma-enhanced chemical vapor deposition with postplasma treatment [J]. Applied Physics Letters, 2005, 87(16): 163123.
- [25] CHEN Y J, XUE X Y, WANG Y G, WANG T H. Synthesis and ethanol sensing characteristics of single crystalline SnO₂ nanorods [J]. Applied Physics Letters, 2005, 87(23): 233101.
- [26] LI Yan, LIU Min. Gas sensing properties of Y-doped ZnO nanosheets synthesized via combustion method [J]. Transactions of Nonferrous Metals Society of China, 2015, 25: 2247–2252.
- [27] ZHENG X J, YI W M, CHEN Y Q, WU Q Y, HE L. The effects of annealing temperature on the properties of Bi_{3.15}Nd_{0.85}Ti₃O₁₂ thin films [J]. Scripta Materialia, 2007, 57: 675–678.
- [28] ZHONG X L, WANG J B, ZHOU Y C, LIU J J, ZHENG X J. Electrical properties of Nd-substituted Bi₄Ti₃O₁₂ thin films fabricated by chemical solution deposition [J]. Journal of Crystal Growth, 2005, 277: 233–237.
- [29] LIN Xue, GUAN Qing-feng, LI Hai-bo, LI Hong-ji, BA Chun-hua, DENG Hai-de. Bi_{3.25}Nd_{0.75}Ti₃O₁₂ nanostructures: Controllable synthesis and visible-light photocatalytic activities [J]. Acta Physico-Chimica Sinica, 2012, 28: 1481–1488.
- [30] ZHONG X L, WANG J B, ZHENG X J, ZHOU Y C, YANG G W. Structure evolution and ferroelectric and dielectric properties of Bi_{3.5}Nd_{0.5}Ti₃O₁₂ thin films under a moderate temperature annealing [J]. Applied Physics Letters, 2004, 85: 5661–5663.
- [31] SEO M H, YUASA M, KIDA T, HUH J S, SHIMANOE K, YAMAZOE N. Gas sensing characteristics and porosity control of nanostructured films composed of TiO₂ nanotubes [J]. Sensor and Actuators B: Chemical, 2009, 137: 513–520.
- [32] LING Hui-qin, LI Ai-dong, WU Di, YU Tao, LIU Zhi-gou, MING Nai-ben. Structure and electrical properties of SrBi₂Ta₂O₉ thin films annealed in different atmosphere [J]. Materials Letter, 2001, 49: 303–307.
- [33] HOU Fang, SHEN Ming-rong, CAO Wen-wu. Ferroelectric properties of neodymium-doped Bi₄Ti₃O₁₂ thin films crystallized in different environments [J]. Thin solid films, 2005, 471: 35–39.
- [34] CHU Xiang-feng, LIU Xing-qin, MENG Guang-yao. The catalytic effect of SmlnO₃ on the gas-sensing properties of CdIn₂O₄ [J]. Materials Science and Engineering: B, 1999, 64: 60–63.
- [35] SHISHIYANU S T, SHISHIYANU T S, LUPAN O I. Sensing characteristics of tin-doped ZnO thin films as NO₂ gas sensor [J]. Sensor and Actuators B: Chemical, 2005, 107: 379–386.
- [36] ZHANG Yong, ZHENG Xue-jun, ZHONG Xiang-li, DENG Shui-feng. The ethanol sensing characteristics of ZnO thin films with low operating temperature synthesized by pulsed laser deposition [J]. Measurement Science & Technology, 2012, 23(10): 105107–105113.
- [37] KAPSE V D, GHOSH S A, RAGHUWANSHI F C, KAPSE S D. Nanocrystalline spinel Ni_{0.6}Zn_{0.4}Fe₂O₄: A novel material for H₂S sensing [J]. Materials Chemistry and Physics, 2009, 113: 638–644.
- [38] WU Li-ming, SONG Fang-fang, FANG Xu-xiong, GUO Zhi-xin, LIANG S. A practical vacuum sensor based on a ZnO nanowire array [J]. Nanotechnology, 2010, 21: 475502–475506.
- [39] ZHANG D, CHAVA S, BERVEN C, LEE S K, DEVITT R, KATKANANT V. Experimental study of electrical properties of ZnO nanowire random networks for gas sensing and electronic devices [J]. Applied Physics A: Materials Science & Processing, 2010, 100: 145–150.
- [40] XU Jia-qiang, CHEN Yu-ping, CHEN Dao-yong, SHEN Jia-nian. Hydrothermal synthesis and gas sensing characters of ZnO nanorods [J]. Sensor and Actuators B: Chemical, 2006, 113: 526–531.
- [41] WANG Li-wei, KANG Yan-fei, LIU Xiang-hong, ZHANG Shou-min, HUANG Wei-ping, WANG Shu-rong. ZnO nanorod gas sensor for ethanol detection [J]. Sensor and Actuators B: Chemical, 2012, 162: 237–243.
- [42] CHIOU B S, LIU K C. Temperature cycling effects between Sn/Pb solder and thick film Pd/Ag conductor metallization [J]. IEEE Transactions on Components Hybrids & Manufacturing Technology, 1991, 14: 233–234.
- [43] STOJANOVIĆ M, HAVERKAMP R G, MIMS C A, MOUDALLAL H, JACOBSON A J. Synthesis and characterization of LaCr_{1-x}Ni_xO₃ perovskite oxide catalysts [J]. Journal of Catalysis, 1997, 166: 315–323.
- [44] WAGHULADE R B, PATIL P P, PASRICHA R. Synthesis and LPG sensing properties of nano-sized cadmium oxide [J]. Talanta, 2007, 72: 594–599.
- [45] EPIFANI M, FRANCIOSO L, SICILIANO P, HELWIG A, MUELLER G, DIAZ R, ARBIOL J, MORANTE J R. SnO₂ thin films from metalorganic precursors: Synthesis, characterization, microelectronic processing and gas-sensing properties [J]. Sensor and Actuators B: Chemical, 2007, 124: 217–226.
- [46] SAKAI G, MATSUNAGA N, SHIMANOE K, YAMAZOE N. Theory of gas-diffusion controlled sensitivity for thin film semiconductor gas sensor [J]. Sensor and Actuators B: Chemical, 2001, 80: 125–131.
- [47] BAIK N S, SAKAI G, SHIMANOE K, MIURA N, YAMAZOE N.

- Hydrothermal treatment of tin oxide sol solution for preparation of thin-film sensor with enhanced thermal stability and gas sensitivity [J]. *Sensor and Actuators B: Chemical*, 2000, 65: 97–100.
- [48] SHIMIZU Y, MAEKAWA T, NAKAMURA Y, EGASHIRA M. Effects of gas diffusivity and reactivity on sensing properties of thick film SnO₂-based sensors [J]. *Sensor and Actuators B: Chemical*, 1998, 46: 163–168.
- [49] SEOA M H, YUASAB M, KIDAB T, SOOHUHC J, SHIMANOEB K, YAMAZOE N. Gas sensing characteristics and porosity control of nanostructured films composed of TiO₂ nanotubes [J]. *Sensor and Actuators B: Chemical*, 2009, 137: 513–520.
- [50] ZHAO Yan, HE Xiu-li, LI Jian-ping, GAO Xiao-guang, JIA Jian. Porous CuO/SnO₂ composite nanofibers fabricated by electrospinning and their H₂S sensing properties [J]. *Sensor and Actuators B: Chemical*, 2012, 165: 82–87.
- [51] ZURUZI A S, MACDONALD N C, MOSKOVITS M, KOLMAKOV A. Metal oxide “nanosponges” as chemical sensors: highly sensitive detection of hydrogen with nanosponge titania [J]. *Angewandte Chemie*, 2007, 119: 4376–4379.
- [52] JING Zhi-hong, ZHAN Jin-hua. Fabrication and gas-sensing properties of porous ZnO nanoplates [J]. *Advanced Materials*, 2008, 20: 4547–4551.
- [53] TIEMANN M. Porous metal oxides as gas sensors [J]. *Chemistry - A European Journal*, 2007, 13: 8376–8388.
- [54] GUO Li-jun, SHEN Xiao-ping, ZHU Guo-xing, CHEN Kang-min. Preparation and gas-sensing performance of In₂O₃ porous nanoplatelets [J]. *Sensor and Actuators B: Chemical*, 2011, 155: 752–758.
- [55] ZHANG Yang, LI Jian-ping, AN Gui-min, HE Xiu-li. Highly porous SnO₂ fibers by electrospinning and oxygen plasma etching and its ethanol-sensing properties [J]. *Sensor and Actuators B: Chemical*, 2010, 144: 43–48.

低工作温度下 Bi_{3.15}Nd_{0.85}Ti₃O₁₂ 薄膜对乙醇的气敏性能

江宏¹, 张勇²

1. 湖南省教育考试院, 长沙 410006;
2. 湘潭大学 物理与光电工程学院, 湘潭 411105

摘要: 利用金属有机物分解法 (MOD), 在 Pt/Ti/SiO₂ 层的 Si (100) 衬底上制备了 Bi_{3.15}Nd_{0.85}Ti₃O₁₂ (BNdT) 薄膜, 并将其分别在氧气氛围和空气中进行快速退火处理。运用 X 射线衍射仪和场发射扫描电子显微镜对 BNdT 薄膜的晶体结构和形貌进行表征, 通过在不同浓度气体氛围下监控材料电阻变化来研究其气敏性能。结果表明, 在空气环境退火的 BNdT 薄膜具有多孔微结构和表面粗糙形貌, 且退火氛围对 BNdT 薄膜气敏性能有较大的影响。在工作温度为 100 °C 时, 在空气中退火的 BNdT 薄膜对 1×10⁻⁶ 乙醇气体具有高的灵敏度, 并且对乙醇气体的极限探测浓度达到 0.1×10⁻⁶。其响应和恢复时间分别约为 6 s 和 10 s。研究结果为制作高性能乙醇传感器有指导的意义。

关键词: BNdT 薄膜; 乙醇气敏性能; 金属有机物分解; 退火气氛; 低工作温度

(Edited by Xiang-qun LI)